Research Square

Preprints are preliminary reports that have not undergone peer review.
They should not be considered conclusive, used to inform clinical practice,
or referenced by the media as validated information.

Diffusion Kurtosis Imaging Evaluates the Neuroprotective Effects of Low-Intensity Treadmill Exercise in a 6-OHDA-Induced Rat Model of Parkinson's Disease

Jie Zhang
First Hospital of Qinhuangdao
Jiajia Gu
Beidaihe Rest and Recuperation Center of PLA
Wenshuang Cao
Beidaihe Rest and Recuperation Center of PLA
Yanchao Dong
First Hospital of Qinhuangdao
Hongzhi Lu
962141865@qq.com

Qinhuangdao Maternity and Child Health Hospital

Article

Keywords: Parkinson's disease, diffusion kurtosis imaging, low-intensity exercise, neuroprotection, substantia nigra

Posted Date: November 10th, 2026

DOI: https://doi.org/10.21203/rs.3.rs-10914817/v1

License: This work is licensed under a Creative Commons Attribution 4.0 International License.
Read Full License

Additional Declarations: No competing interests reported.

Abstract

Parkinson's disease (PD) involves progressive degeneration of dopaminergic neurons in the substantia nigra and abnormal accumulation of α-synuclein (αSyn). Low-intensity exercise has shown neuroprotective potential in experimental PD, yet sensitive in vivo methods for tracking associated microstructural changes remain limited. We therefore used diffusion kurtosis imaging (DKI) to evaluate exercise-associated neuroprotection in 6-OHDA-lesioned rats and examined how DKI metrics related to behavioral and pathological measures. Forty rats were randomly allocated to control, sham, PD, and exercise groups. PD lesions were induced by unilateral 6-OHDA injection into the medial forebrain bundle. The exercise group underwent six weeks of low-intensity treadmill training. After the intervention, SN mean diffusivity (MD), fractional anisotropy (FA), and mean kurtosis (MK) were measured using 3.0-T MRI. Motor performance and SN tyrosine hydroxylase (TH) and αSyn immunoreactivity were assessed, followed by correlation analysis. Compared with control animals, PD rats showed decreased FA and MK, reduced TH immunoreactivity, increased αSyn immunoreactivity, and impaired motor performance. Exercise partially attenuated these abnormalities. FA and MK were strongly associated with behavioral and pathological measures, whereas MD showed no significant group differences. Six weeks of low-intensity treadmill exercise partially ameliorated imaging, behavioral, and pathological abnormalities in 6-OHDA-lesioned rats. The data suggest that FA and MK may serve as candidate non-invasive imaging metrics for assessing nigral injury and monitoring exercise-associated treatment responses in this model.

1 Introduction

Parkinson's disease (PD) is a progressive neurodegenerative disorder characterized by selective degeneration of dopaminergic neurons in the substantia nigra (SN) and abnormal accumulation of α-synuclein (αSyn), leading to motor and non-motor symptoms [1, 2]. Dopaminergic replacement remains the mainstay of treatment. Although it improves symptoms, it does not halt disease progression and may lead to motor complications with prolonged use [3]. Against this background, exercise has attracted interest as a relatively safe adjunctive strategy that may improve motor performance while also influencing disease-related biological processes [1, 3].

Evidence from rodent studies supports a beneficial effect of treadmill exercise in experimental PD. In unilateral 6-hydroxydopamine(6-OHDA)-lesioned rats, low-intensity treadmill training at 5–12 m/min for 20–30 min/day has produced greater neurobehavioral benefits than high-intensity treadmill exercise or swimming [3]. Proposed mechanisms include improved mitochondrial function in the brain and skeletal muscle, attenuation of oxidative stress and neuroinflammation, preservation of dopaminergic tissue, and reduced pathological spread of αSyn [1, 2, 4]. Most of these observations, however, have been derived from terminal histological analyses and behavioral tests. Sensitive non-invasive methods for tracking cerebral microstructural changes in vivo remain limited.

Diffusion tensor imaging (DTI) models water diffusion under an approximate Gaussian assumption, which may reduce its sensitivity to the complex microarchitecture of neural tissue [5]. Diffusion kurtosis imaging (DKI) extends diffusion MRI by quantifying non-Gaussian diffusion and may therefore provide additional information on tissue complexity [6, 7]. n patients with PD, DKI-derived metrics, including mean diffusivity (MD), fractional anisotropy (FA), and mean kurtosis (MK), have revealed microstructural abnormalities in motor-related pathways and have been associated with motor impairment [8]. Similar changes have been detected in mitochondrial permeability transition pore (MPTP)-based mouse models [9]. High-gradient diffusion MRI studies also suggest that advanced diffusion approaches can capture microstructural alterations that are not readily detected by conventional DTI or macroscopic measures [5].

Low-intensity treadmill exercise has shown neuroprotective effects in 6-OHDA-lesioned rats [2], but exercise-associated changes in SN microstructure have not been systematically examined in vivo with DKI. We therefore combined DKI, motor testing, and postmortem immunohistochemistry. The study was designed to assess the effects of low-intensity treadmill exercise on motor dysfunction, quantify SN alterations using MD, FA, and MK, and examine the relationships of these imaging metrics with motor performance, TH immunoreactivity, and αSyn immunoreactivity. This multimodal approach was used to evaluate whether DKI could serve as a non-invasive method for monitoring exercise-associated responses in experimental PD.

2 Materials and Methods

2.1 Animals

Forty male Sprague–Dawley rats (7 weeks old; body weight, 270 ± 10 g) were obtained from Beijing Vital River Laboratory Animal Technology Co., Ltd. (China). The experimental protocol was approved by the Ethics Committee of the First Hospital of Qinhuangdao (approval no. 2024K-021-02). Rats were housed individually at the Laboratory Animal Center of Yanshan University under a 12-h light/dark cycle, a temperature of 22–24°C, and relative humidity of 60 ± 5%, with standard chow and sterile water available ad libitum.

2.2 Study Design and 6-OHDA Lesioning

Rats were randomly assigned to four groups (n = 10 per group): normal control (NC; no cranial surgery), sham-operated (Sham), 6-OHDA-lesioned PD model (PD), and low-intensity treadmill exercise (Exercise). Rats in the PD and Exercise groups received unilateral 6-OHDA injections, whereas Sham rats received vehicle injections using the same stereotaxic procedure.

Anesthesia was induced with 1% Sodium pentobarbital (4ml/kg, intraperitoneally), with additional doses of 1mL/kg/h administered during surgery. Rats were secured in a stereotaxic frame. After a midline scalp incision, a burr hole was made at coordinates targeting the right SN (relative to bregma; anteroposterior, − 4.8 mm; mediolateral, + 1.9 mm; dorsoventral, − 8.0 mm from skull) according to the

rat brain atlas. A Hamilton microsyringe was used to inject 6 μL of 6-OHDA (2 μg/μL in normal saline containing 0.2% ascorbic acid; Sigma, USA) into the right SN of rats in the PD and Exercise groups. No pretreatment for noradrenergic neuron protection was administered [10]. The needle was retained in place for 5 min to minimize reflux, after which the scalp was sutured and intramuscular antibiotic prophylaxis was administered. Sham rats received an equal volume of vehicle at the same coordinates using identical surgical procedures.

Animals were monitored daily from recovery from anesthesia until tissue collection. Spontaneous activity, fur condition, and surgical wound reactions, including swelling, erythema, and scratching, were recorded. No severe surgical wound complications were observed.

2.3 Apomorphine-Induced Rotation Test

Two weeks after lesioning, rats in the PD and Exercise groups received apomorphine (0.5 mg/kg, intraperitoneally) for model verification. After 10 min of acclimation in a quiet cylindrical container, contralateral rotations were recorded continuously for 30 min, beginning 2 min after apomorphine administration. Rats with a mean contralateral rotation rate > 7 turns/min were considered to have successful lesions and were included in subsequent analyses.

2.4 Low-Intensity Treadmill Exercise Protocol

The treadmill protocol was adapted from published exercise studies in rodent PD models [2, 11]. Before lesioning, all rats underwent a 7-day treadmill familiarization period: 3 days at 5 m/min for 10–15 min/day, followed by 4 days of progressive training to 10 m/min. No exercise was performed during the first postoperative week to allow recovery.

Only rats in the Exercise group underwent the intervention for six consecutive weeks, 5 days/week. Each session consisted of a 5-min warm-up at 5 m/min followed by 30 min of continuous running at 10 m/min and 0° incline. Mild electrical stimulation (25–30 V, 0.2 mA) was used only when necessary to encourage running.

2.5 MRI Acquisition and Image Processing

All rats underwent brain MRI at week 7 after lesioning using a 3.0-T Siemens Magnetom Verio (Siemens Medical Solutions, Erlangen, Germany) scanner equipped with an eight-channel coil(Shenzhen Teshen Electric, Shenzhen, China). Scans with visible head motion were repeated 2 h later after additional anesthesia. Axial T2-weighted images were acquired using the following parameters: repetition time (TR), 4000 ms; echo time (TE), 113 ms; flip angle, 150°; number of averages, 6; field of view (FOV), 80 × 80 mm^2; voxel size, 0.3 × 0.3 × 2.0 mm^3; slice thickness, 2.0 mm; 10 slices; acquisition time, 3 min 18 s. The imaging plane was aligned parallel to the anterior–posterior axis of the brain. DKI parameters were: TR, 2000 ms; TE, 107 ms; flip angle, 180°; FOV, 144 × 144 mm^2; slice thickness, 2 mm; 10 slices; reported voxel size, 2.3 × 2.3 × 2 mm^3; matrix, 64 × 64; parallel imaging factor, 2; 30 non-collinear diffusion directions; b values, 0, 1000, and 2000 s/mm^2; acquisition time, 11 min 2 s.

DKI datasets were processed using the Diffusional Kurtosis Estimator toolbox implemented in MATLAB R2017a. Before quantitative analysis, diffusion-weighted images were reviewed sequentially to identify residual motion-related slice misalignment or signal instability. MD, FA, and MK maps were subsequently generated from the accepted datasets. The parametric maps were co-registered with the corresponding T2-weighted images to improve anatomical localization of the SN. Registration quality was checked visually by comparing the contours of the midbrain, cerebral peduncles, and adjacent ventricular and cisternal landmarks across the T2-weighted and parametric images. Datasets showing evident misregistration at the SN level were realigned before ROI measurement.

The right SN was identified on the co-registered T2-weighted and DKI parametric images using anatomical landmarks at matched midbrain levels. Regions of interest (ROI) delineation was occasionally difficult because of the small size of the rat SN, the relatively limited spatial resolution of the clinical 3.0-T scanner, and partial-volume effects at the borders of the cerebral peduncle and surrounding midbrain tissue. To reduce measurement variability, the T2-weighted image was used as the primary anatomical reference, while the MD, FA, and MK maps were viewed simultaneously during ROI placement.

Two radiologists, each with 10 years of experience in neurological MRI, independently delineated circular ROIs on the right SN while blinded to group allocation and behavioral and pathological results. ROIs were placed within the visible boundaries of the SN (0.30–0.60 mm^2) and were kept away from the cerebral peduncle, adjacent cerebrospinal fluid spaces, image edges, and voxels affected by visible artifacts. The ROI position and size were kept as consistent as possible across MD, FA, and MK maps by transferring the ROI between co-registered images rather than redrawing it independently on each parametric map.

When the SN boundary was indistinct, each reader referred to the corresponding T2-weighted image and adjacent slices to determine the most anatomically appropriate location. If the two initial ROIs showed obvious spatial disagreement, both readers jointly reviewed the anatomical landmarks and reached a consensus position without access to the experimental group information. The measurements obtained independently by the two readers were used to calculate the intraclass correlation coefficient (ICC), with an ICC threshold above 0.85 defined as good inter-rater consistency. The mean of the two measurements was used for statistical analysis.

All MRI datasets were visually assessed before postprocessing. Slight motion artifacts were accepted only when they did not involve the SN or interfere with anatomical localization. Images with substantial head displacement, ghosting, signal dropout, or midbrain distortion were excluded from the initial acquisition and repeated after repositioning and supplementary anesthesia. Registration between T2-weighted images and DKI maps was visually verified using midbrain anatomical landmarks.

2.6 Wire Grip Suspension Test

The wire grip suspension test was performed at week 7 after lesioning, following completion of the six-week treadmill intervention, to assess motor coordination and neuromuscular performance [12]. A

horizontal steel wire (60 cm long; 7 mm in diameter) was positioned 1 m above a padded surface. Each rat was suspended by both forepaws, and suspension time was recorded using a stopwatch. After three familiarization trials, each rat completed one formal trial. Testing order was randomized.

2.7 Immunohistochemistry

After MRI, all animals were euthanized at the end of the experiment via intraperitoneal injection of an overdose of sodium pentobarbital (100 mg/kg). Euthanasia was verified by the permanent cessation of breathing and absence of the pedal withdrawal reflex before brain tissue collection. Coronal sections (8 μm) of the ventral mesencephalon were prepared for TH and αSyn immunohistochemistry, and anatomically matched SN levels were selected across groups. Sections were incubated overnight at 4°C with rabbit anti-rat TH and anti-αSyn primary antibodies (Abcam, UK; 1:300), followed by horseradish peroxidase-conjugated secondary antibodies for 30 min at 37°C. Immunoreactivity was visualized using 3,3'-diaminobenzidine, followed by nuclear counterstaining.

Integrated optical density per stained area (IOD/Area) was measured under blinded conditions using Image-Pro Plus 6.0. Four randomly selected fields at 20 × magnification were captured from SN sections of each rat under identical microscope settings. Images underwent rolling-ball background subtraction (radius, 50 pixels) and Gaussian smoothing ($\sigma = 1.0$). Otsu automatic thresholding with manual correction was used to exclude non-specific staining, and particles < 50 μm^2 were removed as noise. The mean IOD/Area of positive staining was calculated for each animal.

2.8 Statistical Analysis

Statistical analyses were performed using GraphPad Prism 9.0 and SPSS 26.0. Normality and homogeneity of variance were assessed using the Shapiro–Wilk and Levene tests, respectively. Data are presented as mean ± standard deviation, with n = 10 per group. Overall group differences were evaluated using one-way analysis of variance, followed by Tukey's post hoc test when the omnibus P value was < 0.05. Pearson correlation analysis was used to examine associations among DKI metrics, suspension time, and SN TH and αSyn IOD/Area. All tests were two-sided, and $P < 0.05$ was considered statistically significant. Inter-rater reliability of MRI measurements was assessed using ICCs.

3 Results

3.1 SN DKI Parameters

Two weeks after lesion induction, rats in the PD and Exercise groups exhibited apomorphine-induced contralateral rotation rates exceeding 7 turns/min and were retained for subsequent analyses. The intraclass correlation coefficients for MD, FA, and MK measurements were 0.928, 0.817, and 0.970, respectively. MR images are shown in Fig. 1A.

One-way analysis of variance showed significant overall group differences in SN FA ($F = 123.9$, $p < 0.0001$) and MK ($F = 72.82$, $p < 0.0001$), whereas MD did not differ significantly among groups. No

pairwise MD comparison was significant (all $p > 0.05$, Fig. 1B). FA did not differ between NC and Sham rats ($p = 0.646$). FA was lower in the PD group than in the NC, Sham, and Exercise groups (all $p < 0.0001$). Exercise increased FA relative to the PD group ($p < 0.0001$), although FA remained lower than in the NC and Sham groups (both $p < 0.0001$, Fig. 1C). MK did not differ between NC and Sham rats ($p = 0.973$). MK was lower in the PD group than in the NC, Sham, and Exercise groups (all $p < 0.0001$). Exercise increased MK relative to the PD group ($p < 0.0001$), although MK remained lower than in the NC and Sham groups (both $p < 0.0001$, Fig. 1D). Thus, 6-OHDA lesioning was associated with reduced SN FA and MK, and treadmill exercise partially attenuated these changes; MD did not distinguish the experimental groups.

3.2 Motor Performance

Suspension time differed significantly among groups ($F = 228.1$, $p < 0.0001$). NC and Sham rats did not differ significantly ($p = 0.931$). PD rats had shorter suspension times than NC, Sham, and Exercise rats (all $p < 0.0001$). Exercise increased suspension time relative to the PD group ($p < 0.0001$), although performance remained lower than in the NC and Sham groups (both $p < 0.0001$, Fig. 2). These findings indicate that exercise partially ameliorated lesion-associated motor impairment.

3.3 SN TH and αSyn Immunoreactivity

TH and αSyn IOD/Area differed significantly among groups (TH: $F = 593.3$, $p < 0.0001$; αSyn: $F = 416.4$, $p < 0.0001$). TH immunoreactivity did not differ significantly between NC and Sham rats ($p = 0.2999$). TH IOD/Area was lower in the PD group than in the NC, Sham, and Exercise groups (all $P < 0.0001$). Exercise increased TH immunoreactivity relative to the PD group ($P < 0.0001$), although values remained lower than in the NC and Sham groups (both $P < 0.0001$, Fig. 3A). αSyn immunoreactivity did not differ significantly between NC and Sham rats ($p = 0.935$). The PD group showed higher αSyn IOD/Area than the NC, Sham, and Exercise groups (all $p < 0.0001$). Exercise reduced αSyn immunoreactivity relative to the PD group ($p < 0.0001$), although values remained higher than in the NC and Sham groups (both $p < 0.0001$, Fig. 3B). These findings indicate that exercise was associated with greater preservation of TH immunoreactivity and a lower αSyn burden. Representative immunohistochemical images of TH are shown in Fig. 4, and those of αSyn are presented in Fig. 5.

3.4 Correlations Among DKI, Behavioral, and Histological Measures

MD showed weak or negligible correlations with the other measures (all $|r| < 0.30$). FA and MK were strongly positively correlated ($r = 0.88$). FA correlated positively with suspension time ($r = 0.90$) and TH immunoreactivity ($r = 0.93$) and negatively with αSyn immunoreactivity ($r = -0.94$). MK correlated positively with suspension time ($r = 0.90$) and TH immunoreactivity ($r = 0.92$) and negatively with αSyn immunoreactivity ($r = -0.94$). Suspension time correlated positively with TH IOD/Area ($r = 0.97$) and negatively with αSyn IOD/Area ($r = -0.95$). TH and αSyn immunoreactivity were strongly negatively

correlated (r = − 0.97, Fig. 6). These associations suggest that SN FA and MK reflected behavioral and histological differences more closely than MD in this dataset.

4 Discussion

Using a unilateral 6-OHDA rat model of PD, we combined DKI with motor testing and SN immunohistochemistry to examine the effects of six weeks of low-intensity treadmill exercise. The lesion was accompanied by lower FA and MK, poorer motor performance, reduced TH immunoreactivity, and greater αSyn immunoreactivity. These abnormalities were partially attenuated in exercised rats. Of note, FA and MK tracked the behavioral and pathological measures closely, whereas MD showed neither significant group differences nor meaningful correlations. Taken together, the data support a neuroprotective effect of low-intensity treadmill exercise on nigral injury and suggest that FA and MK may serve as candidate non-invasive imaging metrics for monitoring exercise-associated responses in this model.

4.1 DKI Detects Exercise-Associated Changes in SN Microstructure

The 6-OHDA lesion reduced FA and MK in the SN, while MD remained unchanged. Low-intensity treadmill exercise increased both FA and MK relative to the untreated PD group, but neither measure returned to control values. The imaging pattern therefore points to partial restoration of nigral microstructural organization rather than normalization.

DKI extends conventional diffusion imaging by characterizing non-Gaussian water diffusion in biological tissue. Its metrics are influenced by diffusion restriction and microstructural heterogeneity generated by cellular compartments, membranes, and other tissue barriers [13, 14]. Prior studies have shown that DKI can detect abnormalities in the SN and other PD-related brain regions, although the direction and magnitude of individual parameters vary across anatomical sites and study populations [15, 16]. In the present model, the lower FA and MK values may reflect disruption of the nigral microenvironment after 6-OHDA lesioning. The accompanying loss of TH immunoreactivity, increase in αSyn immunoreactivity, and decline in motor performance support this interpretation.

However, DKI metrics are not pathologically specific. Altered diffusional kurtosis may result from neuronal loss, neuritic damage, glial responses, changes in extracellular space, or several of these processes occurring together [13, 14]. The present study therefore cannot determine which of these processes predominantly accounted for the observed imaging changes. The absence of significant MD alterations may indicate that tissue organization changed without a substantial net change in average water diffusivity. Alternatively, concurrent pathological processes may have exerted opposing effects on diffusion magnitude.

The present findings support FA and MK as sensitive measures of nigral abnormalities in this model, consistent with previous applications of DKI in PD [15, 16]. However, the current data do not establish that MK is superior to FA, because both parameters showed similar group differences and correlations. Formal comparisons of standardized effect sizes, reproducibility, and classification performance are required before one metric can be considered more sensitive than the other.

4.2 Low-Intensity Exercise Partially Improves Motor Function

PD rats showed markedly shorter wire suspension times than normal and sham-operated animals, confirming substantial motor impairment after 6-OHDA lesioning. Treadmill exercise significantly improved performance. This result is consistent with a systematic review of treadmill interventions in experimental PD and with a recent study showing that low-intensity treadmill exercise improved neurological and motor outcomes in unilateral 6-OHDA-lesioned rats [1, 17, 18].

Motor performance in the exercise group nevertheless remained below that of the control groups. This incomplete recovery was consistent with the partial normalization of FA, MK, TH, and αSyn measurements. Exercise therefore mitigated, but did not eliminate, lesion-related dysfunction.

The wire grip suspension test requires sustained forelimb grip and coordinated postural control. Accordingly, the observed improvement cannot be attributed solely to recovery of nigrostriatal dopaminergic function. Peripheral adaptations may also have contributed. In a unilateral 6-OHDA rat model, low-intensity treadmill exercise improved skeletal muscle mass, mitochondrial function, and antioxidant defenses in parallel with neurological and motor outcomes [2]. Because muscle structure, mitochondrial function, and fatigue resistance were not assessed in the present study, the relative contributions of central neuroprotection and peripheral conditioning remain uncertain.

4.3 Exercise Preserves the Dopaminergic Phenotype and Reduces αSyn Burden

Immunohistochemistry revealed lower TH and higher αSyn immunoreactivity in PD model rats. Treadmill exercise markedly alleviated both lesions, yet the measured indices still differed from normal and sham animals. As shown in 6-OHDA PD rat studies focused on the gut–brain axis, exercise regulates gut flora and intestinal barrier integrity to modulate systemic and cerebral inflammation, which indirectly protects nigrostriatal dopaminergic neurons and curbs pathological αSyn aggregation, reversing lesion-induced TH downregulation..

Higher TH IOD/Area ratios in exercised rats indicate preserved dopaminergic phenotypes. Still, TH signal intensity cannot serve as an unbiased count of surviving neurons, as shifts in enzyme expression, neurite density or staining strength alter IOD/Area independent of neuronal survival. Ten weeks of low-intensity treadmill training only partially restores TH-positive neurons in the striatum and substantia nigra pars compacta; lesioned-side TH cells remain far fewer than normal controls even after exercise. Exercise

boosts TH levels via direct central protection and gut–brain axis-mediated relief of gut-derived endotoxin leakage and microglial hyperactivation [11]. Our results only confirm preserved TH-positive nigral tissue, rather than a true rise in the total number of surviving dopaminergic neurons.

Exercise also diminished cerebral αSyn immunoreactivity, consistent with prior preclinical reports showing treadmill training reduces brain αSyn levels and halts its spreading [4, 19]. Gut–brain axis research further clarifies this pathological cascade: misfolded αSyn spreads from the gut to the brain through the vagus nerve in a prion-like fashion under PD pathology. Exercise remodels dysbiotic gut microbiota and upregulates tight junction ZO-1 to reduce intestinal leakage and lipopolysaccharide (LPS) translocation, blocking the intestinal source and upward transmission of toxic αSyn. Our immunohistochemistry cannot separate soluble, phosphorylated, oligomeric or fibrillar αSyn, as pan and conformation-specific antibodies bind distinct αSyn variants and Lewy structures [20]. Thus, reduced overall αSyn signal cannot confirm less pathological fibril or oligomer deposition.

Existing research attributes exercise neuroprotection to enhanced mitochondrial and antioxidant function, controlled autophagy, lowered αSyn load and suppressed neuroinflammation [1, 2, 4, 19]. Gut–brain axis findings supplement this mechanistic framework: low-intensity running reduces pro-inflammatory genera such as *Oscillospira*, *Bacteroides*, *Megamonas* and *Alistipes*, raises serum anti-inflammatory *IL-10*, and inhibits *TNF-α*, *IL-6*, *IL-1β* expression in the colon and striatum, mitigating inflammation-triggered neuronal loss and αSyn buildup [11]. While our observations align with these central and gut-brain coupled pathways, we did not test gut microbiota, intestinal barrier proteins or peripheral inflammatory markers directly. This study verifies exercise improves PD-related brain pathology, but the exact molecular and gut–brain signaling routes behind these benefits remain unelucidated.

4.4 FA and MK Are Associated With Pathological and Behavioral Outcomes

FA and MK correlated positively with suspension time and TH immunoreactivity and negatively with αSyn immunoreactivity. By contrast, MD showed only weak or negligible associations with these measures. Animals with better-preserved nigral microstructure therefore also showed better motor performance, greater preservation of the dopaminergic phenotype, and lower αSyn burden.

The agreement among imaging, behavioral, and histological measurements strengthens the biological relevance of the DKI findings. Histological analysis provides tissue-level information but requires animal sacrifice, whereas behavioral testing reflects functional impairment without anatomical specificity. As a non-invasive diffusion MRI approach, DKI may help bridge these assessments by providing in vivo information on tissue microstructural alterations [13, 14].

These correlations should be interpreted cautiously. They do not demonstrate that changes in FA or MK caused the behavioral or pathological improvements. Moreover, because the correlation analyses included animals from experimentally distinct groups, the high coefficients may partly reflect between-

group separation rather than continuous associations within each group. Longitudinal analyses and adequately powered within-group analyses are needed to determine whether FA and MK can predict individual treatment responses.

4.5 Limitations and Future Directions

Several limitations should be acknowledged. First, the modest sample size and exclusive use of young male rats, together with the unilateral 6-OHDA model, limit generalizability and do not fully reproduce the progressive, bilateral, and multisystem features of human PD. Second, MRI was performed only after the intervention using a clinical 3.0 T scanner, which precluded longitudinal assessment and may have introduced partial-volume effects, particularly because imaging was restricted to the substantia nigra. Third, pathological and functional evaluations were relatively limited, relying on semiquantitative IOD/Area measurements and a single motor test; future studies should incorporate stereological and biochemical analyses, broader behavioral assessments, and a healthy exercise group to better clarify the mechanisms and specificity of exercise-related neuroprotection.

5 Conclusion

Six weeks of low-intensity treadmill exercise partially ameliorated SN microstructural abnormalities, motor dysfunction, reduced TH immunoreactivity, and increased αSyn immunoreactivity in 6-OHDA-lesioned rats. FA and MK closely reflected behavioral and pathological differences, whereas MD was comparatively insensitive. These findings support FA and MK as candidate non-invasive imaging metrics of nigral injury and exercise-associated treatment response. Longitudinal, higher-resolution, and independently validated studies are required before these metrics can be translated into predictive biomarkers for individualized exercise monitoring in PD.

Declarations

Availability of Data and Materials

The original contributions presented in this study are included in this article and its supplementary material. Further inquiries can be directed to the corresponding author.

Author contributions

JZ performed the data analysis and visualization and conducted the immunohistochemistry experiments. JJG established the mouse PD model and performed dorsal root ganglion tissue collection. YCD cowrote the first draft. JZ and WSC carried out the behavioral assessments. HZL conceived the study and reviewed the manuscript. All authors contributed to editorial changes in the manuscript. All authors read and approved the final manuscript. All authors have participated sufficiently in the work and agreed to be accountable for all aspects of the work.

Ethics Approval and Consent to Participate

The animal study was approved by Ethics Committee of Qinhuangdao First Hospital (approval no. 2024K-021-02). The study was conducted in accordance with the local legislation and institutional requirements.

Acknowledgment

We gratefully acknowledge the Experimental Center of Yanshan University and The First Hospital of Qinhuangdao for providing experimental facilities and technical support.

Funding

The authors declare that financial support was received for the research and/or publication of this article. This work was supported by the Qinhuangdao S&T Plan Program of China (202401A221).

Conflict of interest

The authors declare that the research was conducted in the absence of any commercial or financial relationships that could be construed as a potential conflict of interest.

References

1. Ferreira, A. F. F., Binda, K. H. & Real, C. C. The effects of treadmill exercise in animal models of Parkinson's disease: A systematic review. *Neurosci. Biobehav Rev.* **131**, 1056–1075 (2021).
2. Tung, Y. T. et al. 10 weeks low intensity treadmill exercise intervention ameliorates motor deficits and sustains muscle mass via decreasing oxidative damage and increasing mitochondria function in a rat model of Parkinson's disease. *Life Sci.* **350**, 122733 (2024).
3. Mehta, N., Luthra, N. S., Corcos, D. M. & Fantuzzi, G. C-reactive protein as the biomarker of choice to monitor the effects of exercise on inflammation in Parkinson's disease. *Front. Immunol.* **14**, 1178448 (2023).
4. Dutta, D. et al. Treadmill exercise reduces alpha-synuclein spreading via PPARalpha. *Cell. Rep.* **40** (2), 111058 (2022).
5. Lee, H. et al. Age-related alterations in human cortical microstructure across the lifespan: Insights from high-gradient diffusion MRI. *Aging Cell.* **23** (11), e14267 (2024).
6. Shang, S. et al. Characterizing microstructural patterns within the cortico-striato-thalamo-cortical circuit in Parkinson's disease. *Prog Neuropsychopharmacol. Biol. Psychiatry*. **135**, 111116 (2024).
7. Farquhar, M. E., Yang, Q. & Vegh, V. Robust, fast and accurate mapping of diffusional mean kurtosis. *Elife* 12. (2024).
8. Wei, X. et al. Alterations of diffusion kurtosis measures in gait-related white matter in the ON-OFF state of Parkinson's disease. *Chin. Med. J. (Engl)*. **138** (9), 1094–1102 (2025).
9. Modi, A. et al. Brain Alterations Linked to the MPTP Mouse Model of Parkinson's Disease Uncovered by Diffusion Kurtosis Imaging and Magnetic Resonance Spectroscopy. *CNS Neurosci. Ther.* **32** (4),

e70846 (2026).

10. Boi, L. et al. Serotonergic and dopaminergic neurons in the dorsal raphe are differentially altered in a mouse model for parkinsonism. *Elife* 12. (2024).
11. Tung, Y. T. et al. Therapeutic Effects of Low-Intensity Treadmill Exercise on Motor and Non-Motor Symptoms in a 6-Hydroxydopamine (OHDA) Rat Model of Parkinson's Disease via Gut-Brain Axis Modulation. *Mol. Neurobiol.* **63** (1), 361 (2026).
12. Hadadianpour, Z. et al. The effect of orexin-A on motor and cognitive functions in a rat model of Parkinson's disease. *Neurol. Res.* **39** (9), 845–851 (2017).
13. Jensen, J. H., Helpern, J. A., Ramani, A., Lu, H. & Kaczynski, K. Diffusional kurtosis imaging: the quantification of non-gaussian water diffusion by means of magnetic resonance imaging. *Magn. Reson. Med.* **53** (6), 1432–1440 (2005).
14. Jensen, J. H. & Helpern, J. A. MRI quantification of non-Gaussian water diffusion by kurtosis analysis. *NMR Biomed.* **23** (7), 698–710 (2010).
15. Kamagata, K. et al. A preliminary diffusional kurtosis imaging study of Parkinson disease: comparison with conventional diffusion tensor imaging. *Neuroradiology* **56** (3), 251–258 (2014).
16. Guan, J. et al. Diffusion Kurtosis Imaging for Detection of Early Brain Changes in Parkinson's Disease. *Front. Neurol.* **10**, 1285 (2019).
17. Ishaq, S., Shah, I. A., Lee, S. D. & Wu, B. T. Effects of exercise training on the nigrostriatal glutamatergic pathway and receptor interactions in Parkinson's disease: a systematic review. *Front. Aging Neurosci.* **17**, 1512278 (2025).
18. Ishaq, S., Shah, I. A., Lee, S. D. & Wu, B. T. Effects of exercise training on nigrostriatal neuroprotection in Parkinson's disease: a systematic review. *Front. Neurosci.* **18**, 1464168 (2024).
19. Koo, J. H. & Cho, J. Y. Treadmill Exercise Attenuates alpha-Synuclein Levels by Promoting Mitochondrial Function and Autophagy Possibly via SIRT1 in the Chronic MPTP/P-Induced Mouse Model of Parkinson's Disease. *Neurotox. Res.* **32** (3), 473–486 (2017).
20. Vaikath, N. N. et al. Generation and characterization of novel conformation-specific monoclonal antibodies for alpha-synuclein pathology. *Neurobiol. Dis.* **79**, 81–99 (2015).

Figures

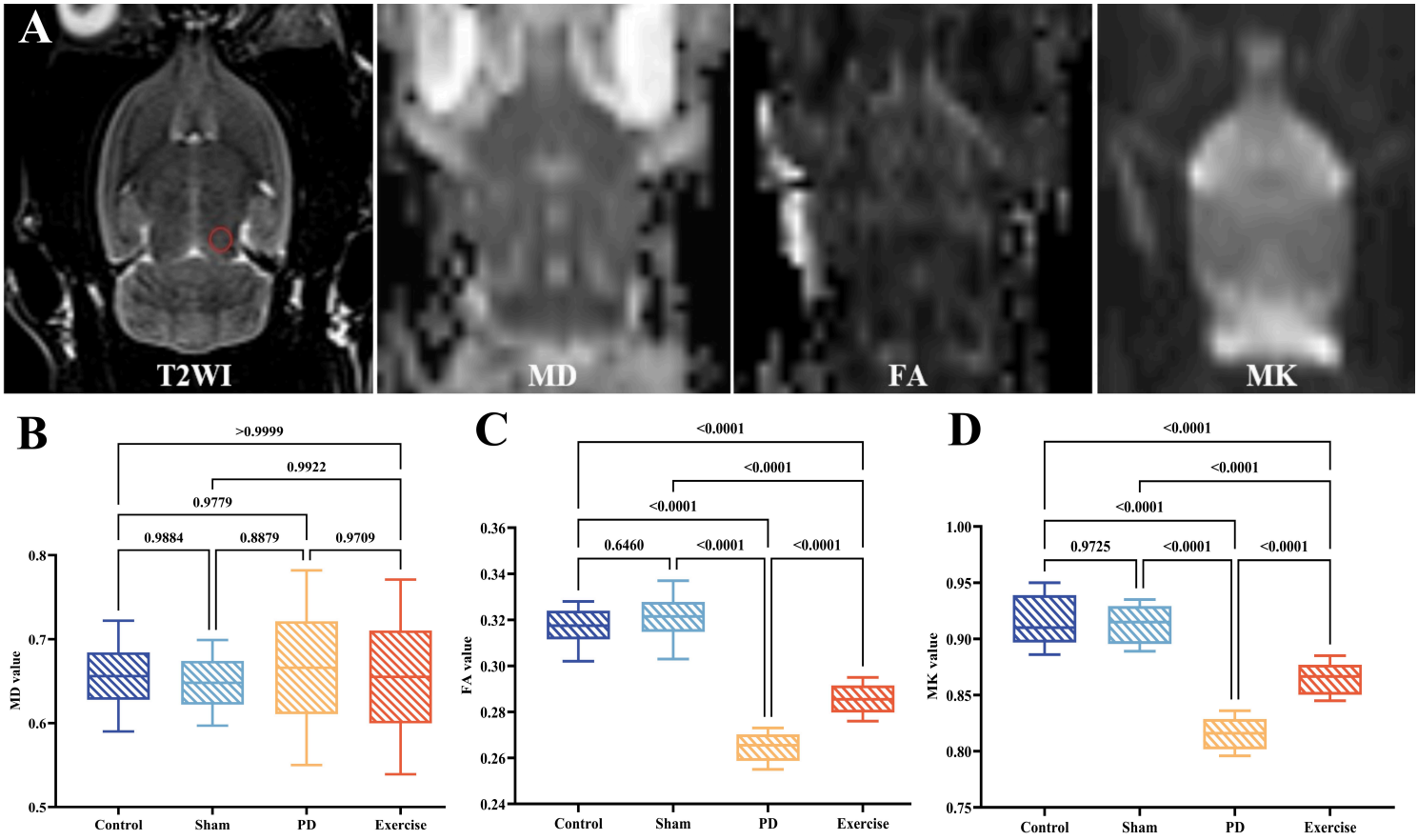


Figure 1

(A) Representative axial T2-weighted image and corresponding mean diffusivity (MD), fractional anisotropy (FA), and mean kurtosis (MK) maps. The red circle indicates the region of interest in the substantia nigra. (B–D) Box-and-whisker plots of SN MD, FA, and MK, respectively, in the Control, Sham, PD, and Exercise groups. Adjusted p values for pairwise comparisons are shown above the brackets.

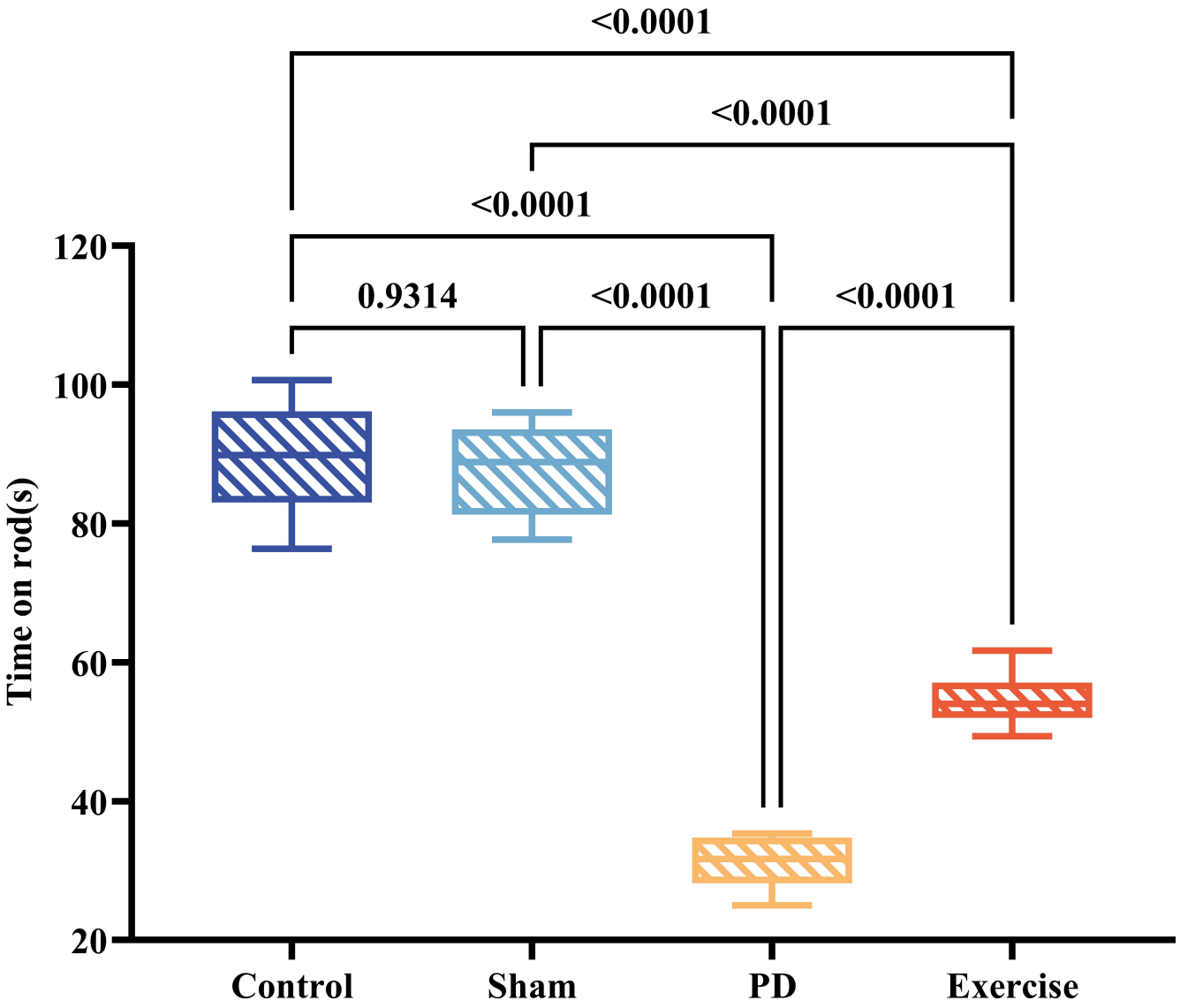


Figure 2

Box-and-whisker plots of suspension time in the wire grip test across the NC, Sham, PD, and Exercise groups. Adjusted p values from one-way ANOVA with Tukey's post-hoc test are shown. n = 10 per group.

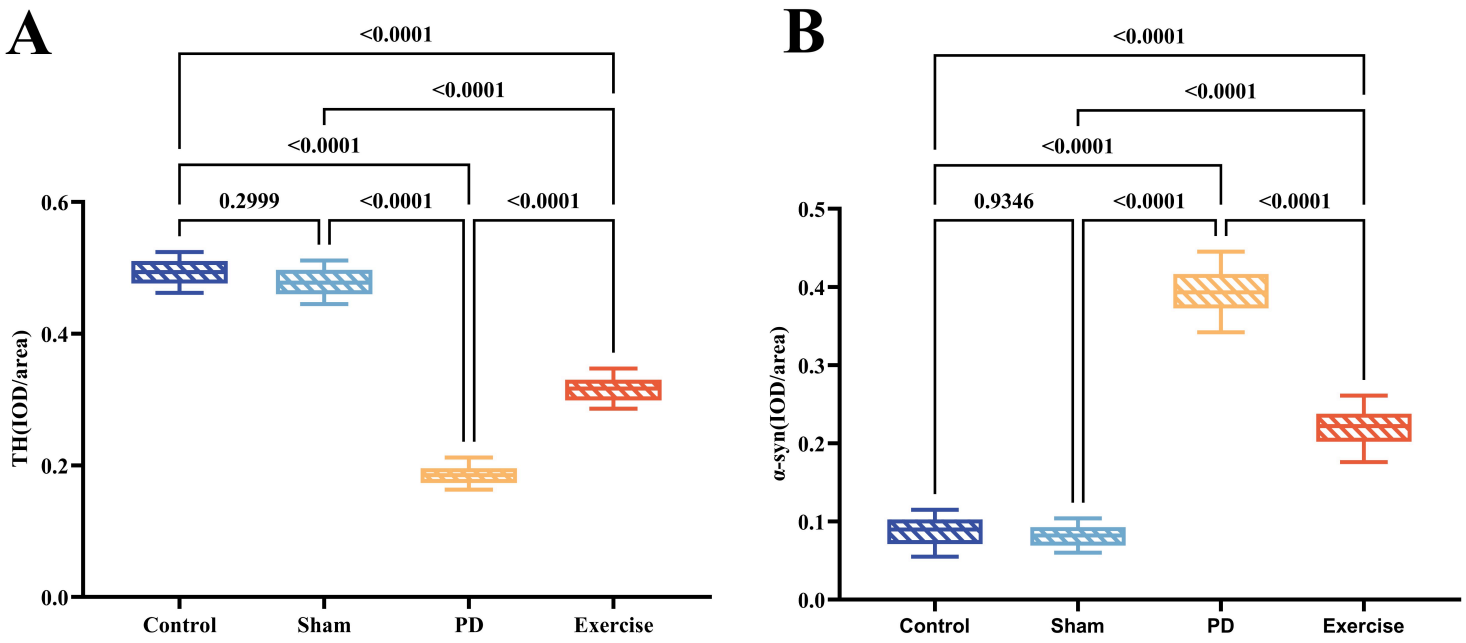


Figure 3

Box-and-whisker plots of (A) α-synuclein and (B) tyrosine hydroxylase (TH) immunoreactivity, expressed as IOD/Area, in the NC, Sham, PD, and Exercise groups. Adjusted p values from one-way ANOVA with Tukey's post-hoc test are shown. n = 10 per group.

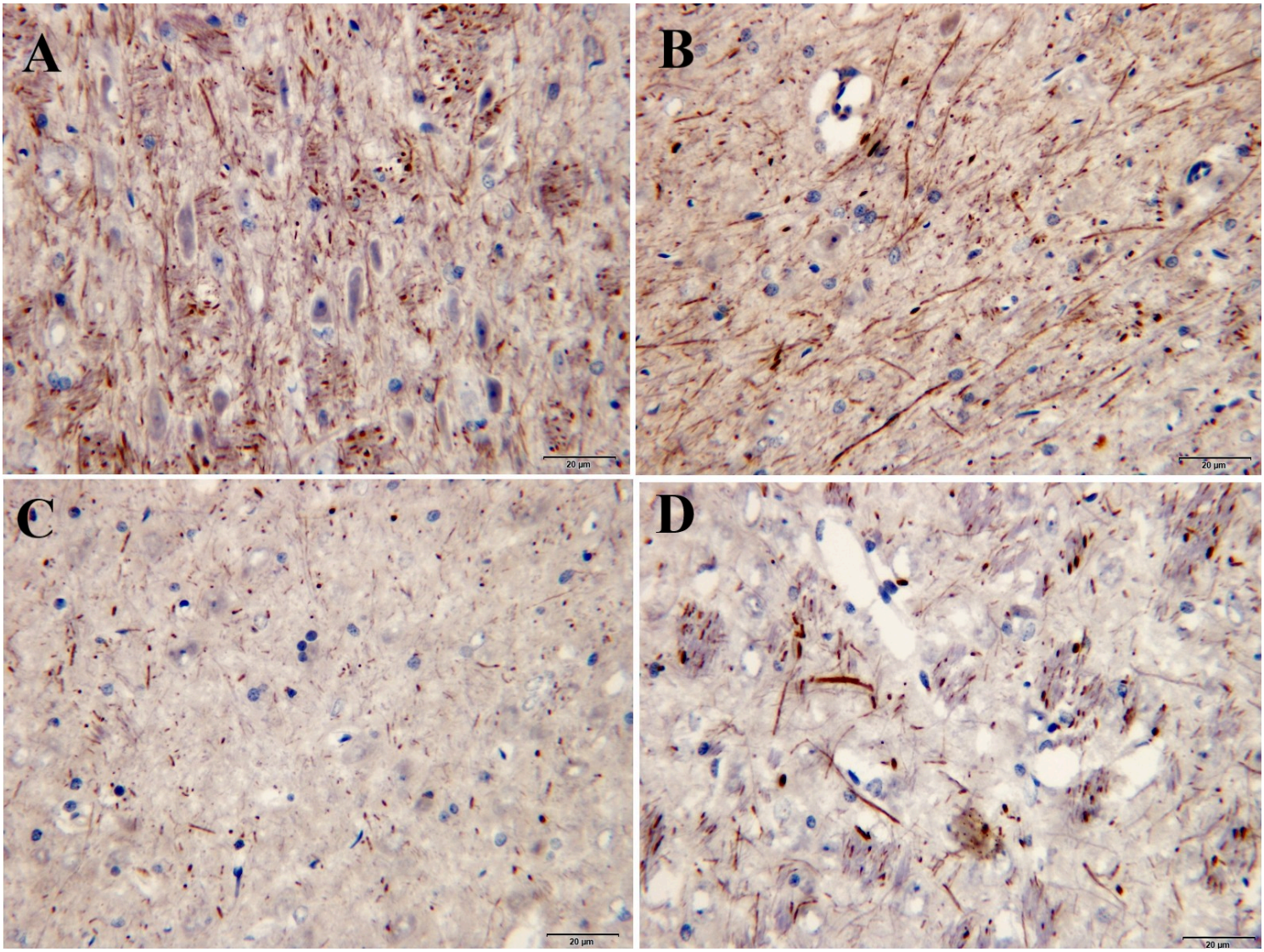


Figure 4

Representative tyrosine hydroxylase (TH) immunohistochemical images of the substantia nigra in the (A) Control, (B) Sham, (C) PD, and (D) Exercise groups. Brown staining indicates TH immunoreactivity, and nuclei are counterstained blue. Scale bar = 20 µm.

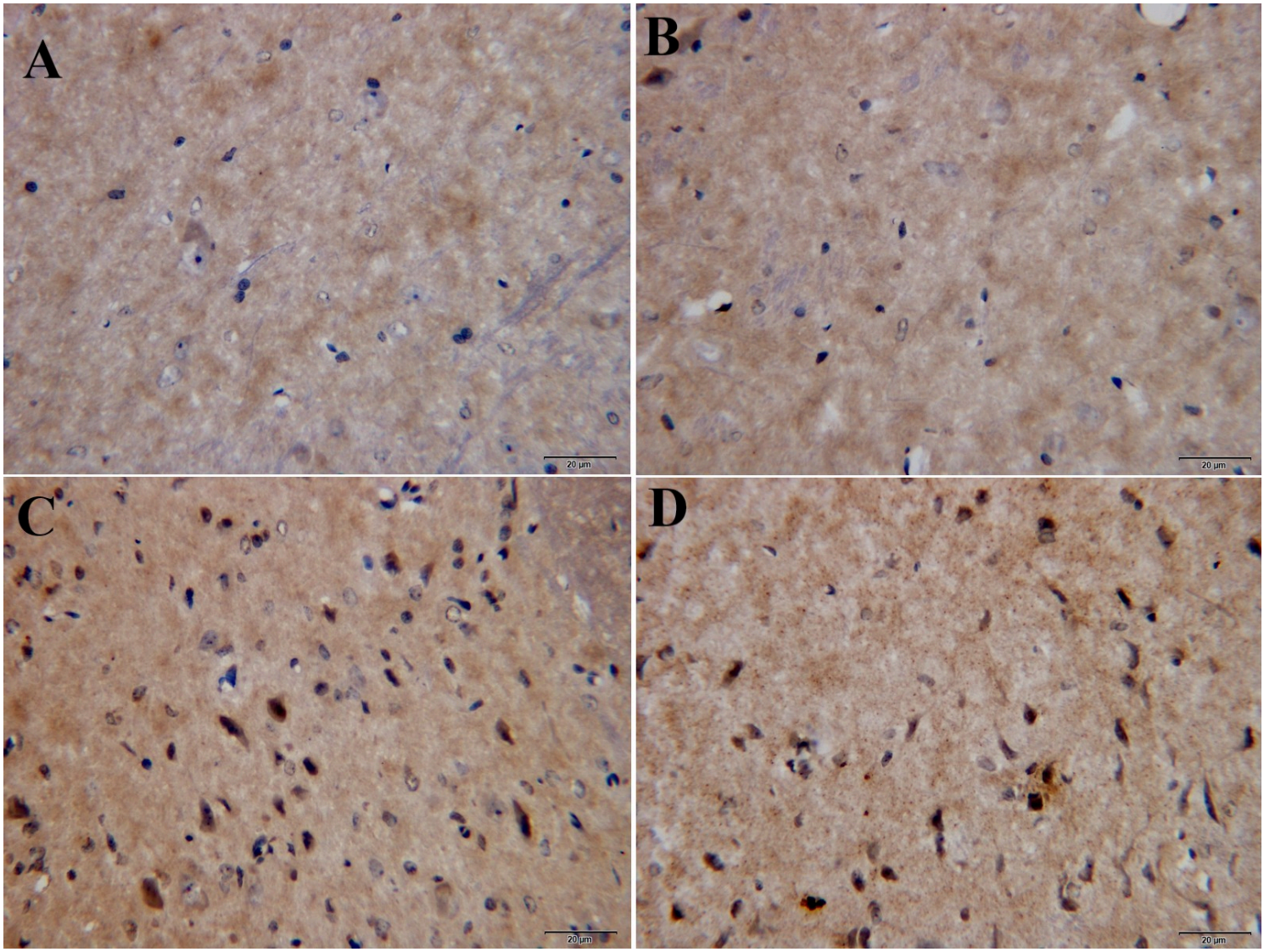


Figure 5

Representative α-synuclein immunohistochemical images of the substantia nigra in the (A) Control, (B) Sham, (C) PD, and (D) Exercise groups. Brown staining indicates α-synuclein immunoreactivity, and nuclei are counterstained blue. Scale bar = 20 μm.

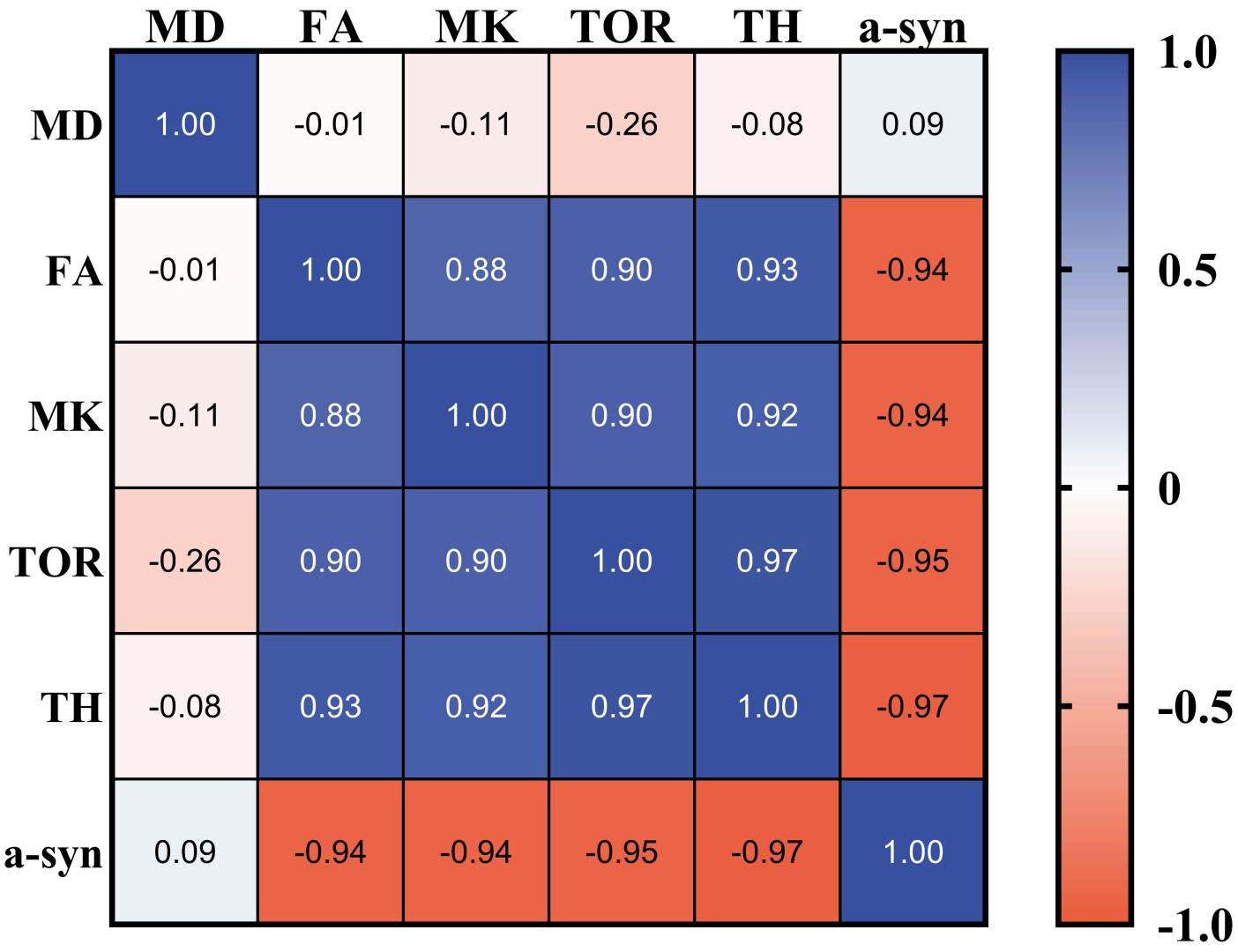


Figure 6

Pearson correlation matrix among MD, FA, MK, time on rod (TOR), TH IOD/Area, and α-synuclein IOD/Area. Values indicate Pearson's r; blue and red denote positive and negative correlations, respectively

Supplementary Files

This is a list of supplementary files associated with this preprint. Click to download.

- 202608131952.mp4